

Cite this: *Mater. Adv.*, 2023,
4, 5003Received 27th July 2023,
Accepted 29th September 2023

DOI: 10.1039/d3ma00472d

rsc.li/materials-advances

Recent advances in targeted nanoparticle drug delivery systems for ischaemic stroke

Xiaojun Li,^{†a} Qi Wang,^{†b} Qi Fang,^{†c} Jianling Xu,^a Baosong Han,^d Yongquan Chen,^a Weidong Yao,^{*a} Sheng Ye^{id} ^{*e} and Bin Wang^{*a}

Ischaemic stroke (IS) is the second most common cause of death worldwide. Traditional treatment strategies, including blood flow recanalization therapy and neuroprotective drugs, have reduced safety and effectiveness due to their lack of targeting and inability to penetrate the blood–brain barrier (BBB). Targeted nanoparticles (NPs) can improve BBB penetration and brain targeting by changing their composition and structure, which can integrate a variety of treatment components to match the complex pathological process of IS. In this review, we describe recent advances in IS therapy, specifically in the prevention, detection, and treatment of IS, by using targeted NPs, presenting basic knowledge and possible therapeutic targets to highlight their potential for early treatment in the clinic.

1. Introduction

Ischaemic stroke (IS) is one of the leading causes of death and disability and poses a serious threat to human health.^{1–3} It creates an enormous burden on the family and society.^{4,5} IS is caused by emboli, which result in a sudden decrease in blood flow to the brain.⁶ Ischaemia triggers energy exhaustion and a series of biochemical events, including ionic imbalance and excitotoxicity, oxidative stress, cell death, the complement system, inflammation, and the initiation of immune responses. This eventually leads to brain tissue damage.^{7–9} Existing therapeutic strategies include antithrombotic and neuroprotective strategies.¹⁰ (1) Antithrombotic: drug thrombolysis and surgical thrombolysis are the standard treatments for acute IS.¹¹ However, there is a narrow treatment window¹² and a risk of haemorrhagic transformation (HT).^{13–15} Moreover, reperfusion injury occurs after blood flow recanalization.^{16–19} Ischaemia–reperfusion injury is a pathological condition in which tissue damage and inflammation are exacerbated after restoration of blood flow and oxygenation.²⁰ (2) Neuroprotective drugs: Neuroprotective

drugs can relieve ischaemia–reperfusion injury by fighting inflammation and stress and save the brain tissue of the penumbra around the infarct core area. Although many neuroprotective drugs have been developed, the vast majority have failed to show efficacy because of their poor ability to cross the BBB and target infarcts.^{8,21} Moreover, the limited regenerative ability of brain tissue and the microenvironment that inhibits regeneration after stroke require brain tissue regeneration therapy.²² Brain tissue regeneration can be effectively promoted through the input of cytokines and exogenous stem cells that stimulate endogenous regeneration.²³ Recently, targeted NPs have shown advantages in the treatment of IS.^{24–26} Targeted NPs can be designed to change their structure and composition so that they can bind to ischaemic brain tissue and ultimately enrich the therapeutic component to achieve a therapeutic effect at a low dose.²⁷ This approach reduces the side effects of systemic high doses. The increased targeting allows the drug to reach therapeutic concentrations in the brain without having to cross the BBB in large quantities to exert a therapeutic effect. It can also increase BBB transport and permeability through the intercellular or cell-mediated pathway,²⁸ which increases the amount of drug in the whole brain and can also have therapeutic effects.²³ In addition, targeted NPs can integrate multiple therapeutic components and participate in different pathological processes of IS.⁴² Although ideal targeting NPs with all the above advantages have not yet been developed, targeted NPs have potential for these advantages and therefore have promising prospects. In this review, we first analyse the shortcomings of conventional treatment strategies and conclude that one of the reasons is the lack of targeting and then focus on the application of three types of targeting NPs in the prevention, diagnosis, and treatment of IS by targeting thrombi, ischaemic brain tissue, and the BBB.

^a Department of Anesthesiology, the First Affiliated Hospital of Wannan Medical College, Yijishan Hospital, Wuhu, China. E-mail: yaowdmd@163.com, w1986wb@163.com

^b Department of Neurology, the First Affiliated Hospital of Wannan Medical College, Yijishan Hospital, Wuhu, China

^c Department of Anesthesiology, the First Affiliated Hospital of Anhui Medical University, Hefei, China

^d Department of Emergency, the First Affiliated Hospital of Wannan Medical College, Yijishan Hospital, Wuhu, China

^e College of Science & State Key Laboratory of Tea Plant Biology and Utilization, Anhui Agricultural University, Hefei, China. E-mail: sye503@ahau.edu.cn

[†] These authors contribute equally to this work.



2. Conventional treatment strategies

Conventional treatment strategies for IS mainly include antithrombotic and neuroprotective strategies. Antithrombotic therapy includes antiplatelet drugs and anticoagulant drugs to prevent thrombosis^{30,43,44} and thrombolytic drugs to dissolve already formed thrombosis.^{32,45,46} Neuroprotective agents mainly inhibit glutamate-mediated excitotoxicity,⁴⁰ oxidative stress,^{47,48} and inflammation.^{49,50} The types of conventional treatment strategies are summarized in Table 1. The disadvantages of conventional therapy are the short retention time of the drug in the blood, the lack of targeting, and the need for repeated systemic administration of large doses to achieve effective therapeutic concentrations at the lesion site, which increases the side effects of the drug. Therefore, targeting NPs have been developed.

3. Strategies of targeted NPs in the treatment of IS

The progress of nanotechnology has brought new opportunities for targeted NPs to treat IS. There are three main targeting strategies: passive targeting, active targeting, and stimulus-responsive targeting. Passive targeting can increase retention in blood by modifying nanocarriers. However, due to the lack of specificity, it is difficult for the vector to reach a specific tissue and be released;⁵¹ therefore, active targeting strategies have been proposed. Active targeting has cell or tissue specificity and is achieved by binding active ligands to NPs. This active ligand could bind to a specific ligand that is present in certain cells or tissues, such as P-glycoprotein (P-gp) on microvascular endothelial cells that make up the BBB and an ATP-binding cassette (ABC) that is significantly expressed at the BBB.⁵² Another targeting strategy is stimulus-responsive targeting. Such NPs can release therapeutic components in response to a specific stimulus in the environment.^{53,54} Things like magnetism, light, sound, a certain range of pH, oxidative stress, enzymes. The clinical application of nanotechnology is mainly reflected in diagnosis and treatment.^{55,56} In the following section, we summarize the targeted NPs acting on thrombi, the BBB, and ischaemic brain tissue during the development of IS to achieve early detection and diagnosis of thrombus. At the same time, the effective therapeutic components of the drug cross the BBB and reach the lesion site of IS to exert a therapeutic effect. Although there are no targeted NPs that can meet the above comprehensive therapeutic effects, with the progress of science and technology, the improvement of manufacturing level, and more in-

depth and continuous research on the pathological mechanism of IS, targeted NPs have broad prospects in the treatment of IS (Fig. 1). Table 2 summarizes the strategies of targeted NPs in the treatment of IS.

4. Targeted NPs for the diagnosis and treatment of thrombosis

Thrombosis is a major cause of IS; therefore, NPs targeting thrombosis could be a therapeutic strategy to treat IS.

4.1 Magnetic NPs

Magnetic nanoparticles, especially iron oxide nanoparticles, have been widely used in biomedicine over the past two decades.⁶⁹ Iron oxide nanoparticles (IONPs) are potential magnetic resonance imaging (MRI) contrast agents that can increase the contrast between diseased and normal tissues.⁷⁰ Superparamagnetic properties allow them to move under an applied magnetic field, and the nanoparticles also have the ability to load drug components. Magnetic iron oxide nanoparticles (MIONPs) have emerged as a promising therapeutic nanoplatform for brain imaging and drug delivery due to their unique physical properties and nontoxic, biodegradable properties. Atherosclerosis is one of the most important causes of stroke. There is no doubt that the early detection of problem vessels and early intervention are very important. Angiogenic biomarkers, such as $\alpha_v\beta_3$, are highly induced in early diseased vessels and have become our targets for detecting early diseased vessels. Winter *et al.* developed a paramagnetic nanoparticle contrast agent that targets $\alpha_v\beta_3$ integrins of angiogenesis in atherosclerotic plaques.⁵⁷ It can detect early diseased vessels and is noninvasive. This experiment was performed at a field strength of 1.5 Tesla, and the enhanced signal on the rabbit aortic wall could be observed, but the layer of the aorta could not be distinguished. With the higher field strength of the application of the MR scanner, higher resolution images can be obtained, which will improve the early patches of positioning and promote clinical risk assessment. In addition, magnetic NPs can be used to track cells and monitor stroke inflammation.^{71,72} Sillerud *et al.* developed novel anti-IBA-1 targeting superparamagnetic iron-platinum (FePt) NPs, which target microglia. The development of neuroinflammation after ischaemic stroke is understood by monitoring the spatiotemporal distribution of microglial/macrophage activation *in vivo* by magnetic resonance imaging.⁵⁸ Magnetic NPs capable of achieving high resolution and high sensitivity have also been reported.^{73,74} Magnetic field-

Table 1 Types of conventional treatment strategies and representative therapeutic agents

Treatment	Therapeutic agent	Mechanism of action	Ref.
Antiplatelet therapy	Aspirin	Inhibits COX-1 involved in platelet adhesion	29 and 30
Anticoagulants	Heparin	Deactivate thrombin and inhibit clotting factors	31 and 32
	Warfarin	Vitamin K antagonist, reduces the production of activated clotting factors	32–34
	Argatroban	Directly inhibits the thrombin	35
Thrombolysis	rTPA, Urokinase	Activate the plasminogen to form plasmin	36
Neuroprotectants	Nimodipine	Calcium channel blocker	37 and 38
	Edaravone	Free radical scavenger	39
	Memantine	NMDAR antagonist	40 and 41



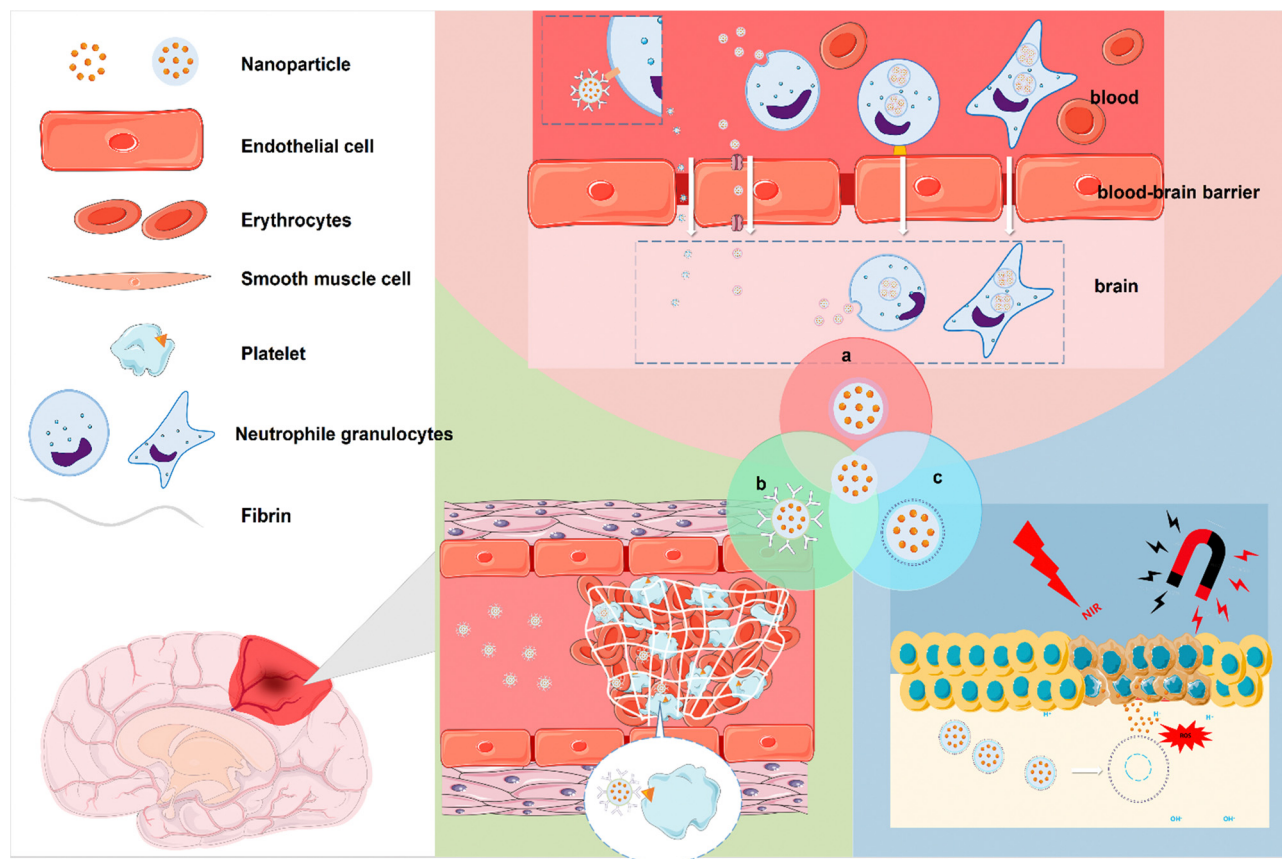


Fig. 1 Schematic images of strategies of targeted NPs in the treatment of IS. (a) Targeted NPs to overcome the BBB. (b) Targeted NPs for the diagnosis and treatment of thrombosis. (c) NPs targeting ischaemic tissue.

responsive NPs can be controlled to accumulate NPs in diseased tissue by simply using an external magnetic field. Hu *et al.* developed a kind of pPMNP-rtPA that integrates rtPA, fibrin-avid peptide and the magnetic nanoparticle PMNP. This magnetic nanoparticle targets fibrin and can be guided by a magnetic field, thus achieving thrombolysis at a low concentration.⁶⁰ By incorporating tPA into porous magnetic iron oxide (Fe_3O_4)-microrods (tPA-MRS), the thrombolytic drug tPA can be targeted to the site of IS caused by distal occlusion of the middle cerebral artery. This NP is rod-like, as observed by scanning electron microscopy (SEM), scanning transmission electron microscopy (STEM) and transmission electron microscopy (TEM). Studies have shown that the intra-arterial injection of tPA-MRS can be targeted to the embolized site in the brain, and tPA is subsequently released under the guidance of an external magnet (Fig. 2). Under the action of an external rotating magnetic field, tPA-MRS can increase the distribution of tPA at the embolization site and can also mechanically destroy the blood clot, which further increases the penetration of tPA. This treatment strategy significantly reduced the time to recanalization of blood flow compared to the tPA treatment group. The downsides of this material are the possibility of endothelial damage and the possibility that a clot that is not destroyed may form another clot in the finer blood vessels downstream. Therefore, further research is necessary. In other reports, L-arginine magnetic NPs wrapped by platelet

membranes can be guided by an external magnetic field and targeted by platelet membranes to the characteristics of the injured tissue, and they can aggregate in ischaemic brain tissue by releasing the vasodilator NO.⁷⁵ In brief, high-resolution imaging depends on magnetic nanoparticles with high magnetic field sensitivity and the field strength provided by the MR scanner, and IONPS as a potential MRI contrast agent needs further investigation. This also limits its application and promotion to some extent.

4.2 Ultrasound-responsive NPs

Ultrasound is considered a nondrug strategy for the treatment of cerebral ischaemia,⁶¹ which is based on the principle that ultrasound generates microbubbles to mechanically destroy thrombi. The created magnetic microvesicles are guided with the help of an external magnetic field to the thrombus area, where ultrasound-mediated tPA release and rupture of the microvesicles lead to thrombolysis. Zhong *et al.* synthesized Fe_3O_4 -PLGA-PFH-CREKA NPs. CREKA (Cys-Arg-Glu-Lys-Ala) specifically targets fibrin, and perfluorohexane (PFH) is a functional reagent that causes a liquid-gas phase transition (PT) (Fig. 3).⁶¹ This NP is shown to be spherical by TEM. Fe and fluorine (F) were confirmed to be present in the NPs by elemental line-scan mapping. The highly biocompatible compound PLGA was used as the carrier. This NP is also responsive



Table 2 Strategies of targeted NPs in the treatment of IS

Type of targeting	Location	NPs	Target	Achievement	Ref.
Active targeting	Thrombus	(PFC) NPs	$\alpha_v\beta_3$ integrins	Detecting and monitoring atherosclerotic plaques	57
Active targeting	Thrombus	(FePt) NPs	Iba-1	Monitoring the dynamic development of neuroinflammation	58
Stimulus-responsive targeting	Thrombus	pPMNP-rtPA		Reduce the clot lysis time	59
Stimulus-responsive targeting	Thrombus	tPA-MRS		Increased clot interaction and penetration of tPA	60
Active targeting	Thrombus	Fe ₃ O ₄ -PLGA-PFH-CREKA NPs	Fibrin	The early noninvasive diagnosis and treatment of arterial thrombosis	61
Passive targeting		CDNPs		The retention time of CD is extended, ultrasound imaging	27
Stimulus-responsive targeting	Ischaemia region	IR-LnNPs		Early assessment of IS	62
Stimulus-responsive targeting	Ischaemia region	t-PA@iRNP	pH-sensitive	Extended the <i>in vivo</i> half-life of t-PA in systemic circulation	63
Stimulus-responsive targeting	Ischaemia region	Ca-MOF@miR-124	pH-sensitive	Enhance the efficacy of NSCs	64
Stimulus-responsive targeting	Ischaemia region	SHP-RBC-NP/NR2B9C	ROS-sensitive	Reduce ischaemic brain damage	42
Stimulus-responsive targeting	Ischaemia region	B-PDEA	ROS-sensitive	Mediates efficient gene transfection of NSCs	65
Stimulus-responsive targeting	Ischaemia region	DGA	ROS-sensitive	Suppressing the translocation of nuclear HMGB1	66
Stimulus-responsive targeting	Ischaemia region	CyBA/PFM NPs	H ₂ O ₂ -sensitive, platelet-targeted	Remove ROS, remove clots	67
Stimulus-responsive targeting	Ischaemia region	ASNPs	MMP-9	Reducing the side effects of systemic gliburide administration	68
Active targeting	BBB	MSNPs	LDLR	Enhance their transcytosis across the BBB	28
Active targeting	BBB	cl PGP-PEG-DGL/CAT-Aco system	neutrophils	Enhance their transcytosis across the BBB	23

to ultrasound and magnetic fields and targets thrombi. It can be used for the early noninvasive diagnosis and treatment of arterial thrombosis and magnetic resonance (MR) and photoacoustic (PA) imaging. This treatment strategy was shown to significantly reduce thrombus volume in a Sprague Dawley (SD) rat abdominal aortic thrombosis model. However, this therapeutic strategy acts by activating the fibrinolytic system rather than inhibiting platelet aggregation, as confirmed by D-dimer, which reflects the degree of fibrinolysis, and P-selectin, which reflects the degree of platelet aggregation. Atherosclerosis is an important cause of IS.^{76,77} Mehta *et al.* developed a system that could deliver 2-hydroxypropyl-beta-cyclodextrin (CD, which dissolves cholesterol and reduces the size of atherosclerotic plaques) NPs (CDNPs) *via* air-trapped polybutylcyanoacrylate NPs (with diameters of 388 ± 34 nm), which significantly increased CD uptake in mouse cells. The contrast agent can be used for ultrasound and near-infrared (NIR) imaging, and ultrasound can also enhance the uptake of NPs by cells.²⁷ Focused ultrasound can increase the entry of therapeutic NPs into brain tissue by increasing the permeability of the BBB. Nance *et al.* tested the increased ability of NPs to penetrate the BBB after temporary and reversible local disruption of the barrier using focused ultrasound (FUS) and intravascular microbubbles (MBs) following MR localization.⁷⁸ Targeted ultrasonic microbubble destruction (UTMD) is a minimally invasive method to open the BBB.⁷⁹ Zhao *et al.* developed PS-containing microbubbles (PS-MBs) that open the BBB through UTMD and then convert to PS-NPs, which are ingested by activated microglia/macrophages (M/M). MBs can be used as a drug carrier-loaded therapy component in the treatment of IS. Safety is still needed to consider problems, including damage to the surrounding tissue and blood clots after fracture potential microthrombus again for distal vascular embolization. Other imaging detection methods need continuous improvement.

5. NPs targeting ischaemic tissue

Pathological processes of IS (such as inflammation, hypoxia, oxidative stress, acidosis, *etc.*) are used as targets for the development of stimulus-responsive biomaterials. These biomaterials can “read” microenvironmental changes in ischaemic tissue and respond in predetermined ways to help alleviate, suppress, and sometimes even reverse symptoms of the disease. How these properties can be used as stimuli to develop smart NPs targeting ischaemic tissue in IS is described next.

5.1 Light-sensitive NPs

Near-infrared light (NIR) can penetrate scalp, skull and brain tissue,^{80–82} and various NPs can be developed to detect and treat IS through the photobiostimulation effect generated by such irradiation.^{83,84} Zhang *et al.* developed a highly reactive oxygen species (HROS) response ratio NIR-II nanoprobe based on the dye sensitization system between IR-783 dyes and lanthanide-doped NPs (IR-LnNPs) (Fig. 4). The probe can distinguish the oxidative stress classification of different regions of the lesion site by responding to HROS. Moreover, IR-II can show ischaemic areas 30 minutes after cerebral ischaemia, long before brain damage can be detected by CT or MRI. The same results were confirmed by staining of tissue sections. Thus, early assessment of IS has been achieved.⁶² Shao *et al.* used the photothermal effect to create erythrocyte membrane-cloaked Janus polymeric motors (EM-JPMs), which were propelled by NIR laser irradiation and successfully applied in thrombus ablation. Adjusting the power of NIR light to control the temperature increases the temperature of photosensitive materials, resulting in the ablation of blood clots. However, NIR irradiation may also damage adjacent tissues.⁸⁵ NPs have also been developed that integrate multiple functions of targeting, thrombolysis, and imaging. Urokinase-type plasminogen activator (Uk) is a kind of thrombolytic drug, but due to its



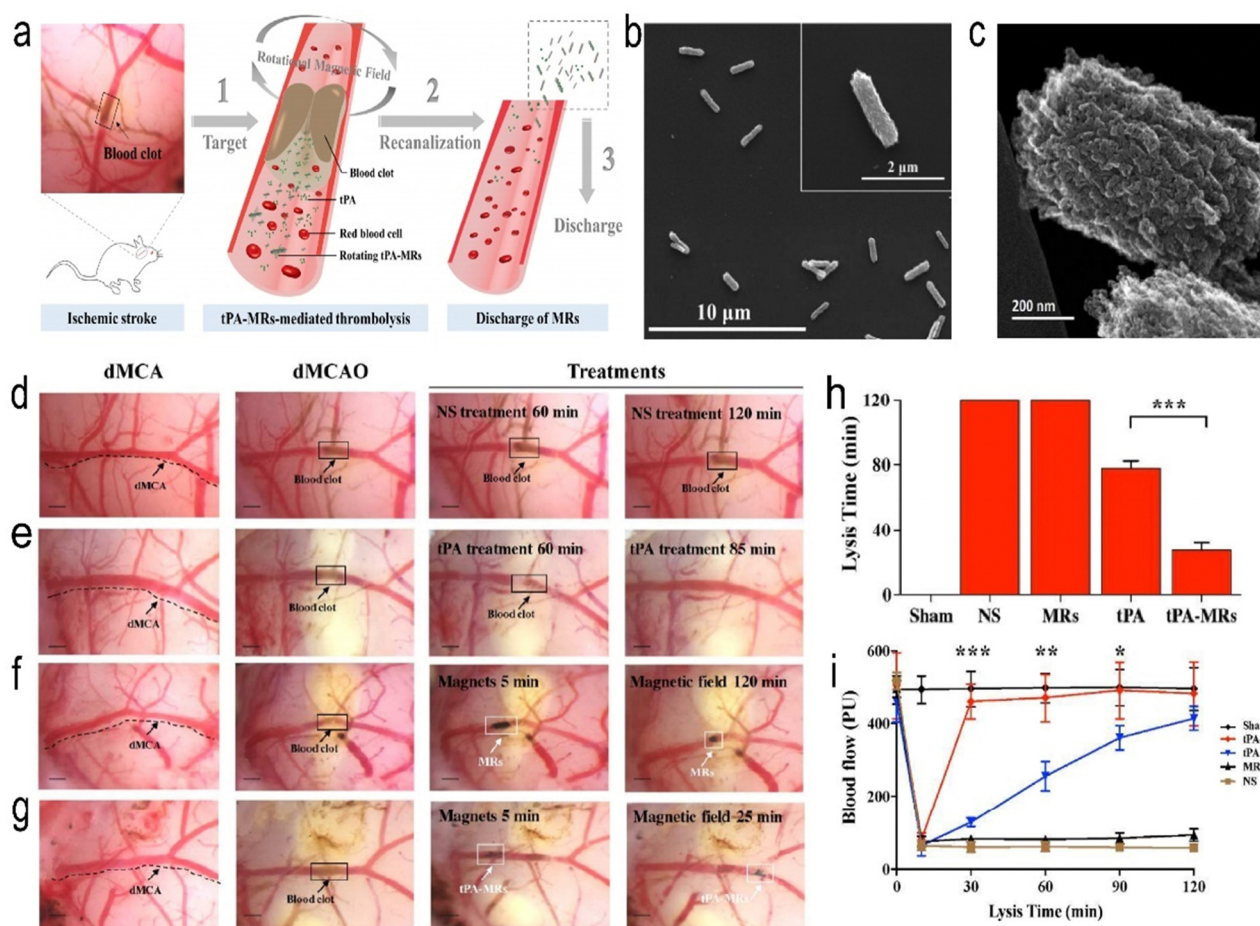


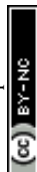
Fig. 2 (a) Schematic representation of the tPA-MR thrombolysis process. (b) SEM images of the $\text{Fe}_3\text{O}_4\text{-C}$ MRs. (c) TEM image of the edge of an $\text{Fe}_3\text{O}_4\text{-C}$ MR. (d) Representative images of thrombolysis in dMCAO mice treated with normal saline (NS). (e) After treatment with tPA, the blood clot was lysed. (f) Representative images of thrombolysis in dMCAO mice. (g) In the tPA-MR solution group, thrombi could be lysed. (h) Plot of lysis time for recanalization in the dMCAO mouse model. (i) Laser Doppler test of dMCA blood flow in sham-operated mice and before and after the formation of thrombi in the dMCA. Reprinted (adapted) with permission from ref. 60. Copyright 2018, American Chemical Society.

nonspecific distribution, it must be used in large doses to increase the concentration at the thrombus to play a role in thrombolysis. However, it also leads to a risk of bleeding. Chang *et al.* developed a multifunctional nanoparticle in which fucoidan (Fu), an alginate-derived anticoagulant, specifically binds to P-selectin, giving the nanoparticle the ability to target the activated platelet thrombus site. The nanoparticles also contained indocyanine green (ICG), a near-infrared (NIR) fluorescence imaging contrast agent, which was incorporated into arginine peptide-functionalized mesoporous silicon-coated gold nanorods (photothermal Si-AuNRs). This nanocomposite has multiple functions, including thrombolytic targeted drug delivery, photothermal thrombolysis, and near-infrared fluorescence imaging, and is therefore an advanced thrombolytic therapy platform to reduce bleeding risk and improve imaging/thrombolysis efficiency. These composite nanomaterials have a variety of functions, including the ability to target activated platelets at the site of the thrombus for rapid removal and prevention of thrombus reformation, while imaging capabilities allow them to monitor the efficacy of thrombolysis, making them promising targeted NPs.⁸⁶ Although near-infrared

light penetration is good, it is still limited, and the deeper tissue effect is poorer. Near-infrared light irradiation *in vitro* is only an approximate range that cannot be accurately achieved, so photosensitive nanoparticle targeting is particularly important; otherwise, it will damage adjacent tissues, and a more controllable thermal effect of the material needs to be developed.

5.2 pH-responsive NPs

Low pH in ischaemic brain tissue can be the target of targeted NPs. In IS, the lack of oxygen supply at the ischaemic site causes tissue metabolism to switch from aerobic to anaerobic, resulting in lactic acid build-up and a decrease in pH that can be used to guide pH-targeting NPs. Yao *et al.* prepared a pH-responsive fluorescent liposome probe (BOD@Lip) that combines the benefits of near-infrared fluorescence (NIRF) and targeting ischaemic tissue. It can enable the observation of ischaemic brain tissue in real time with high sensitivity and high resolution, providing a basis for clinicians to adopt timely and accurate treatment.⁸⁷ Cheng *et al.* designed a pH-sensitive RAPA NP system that enhances magnetic resonance imaging (MRI) and NIRF



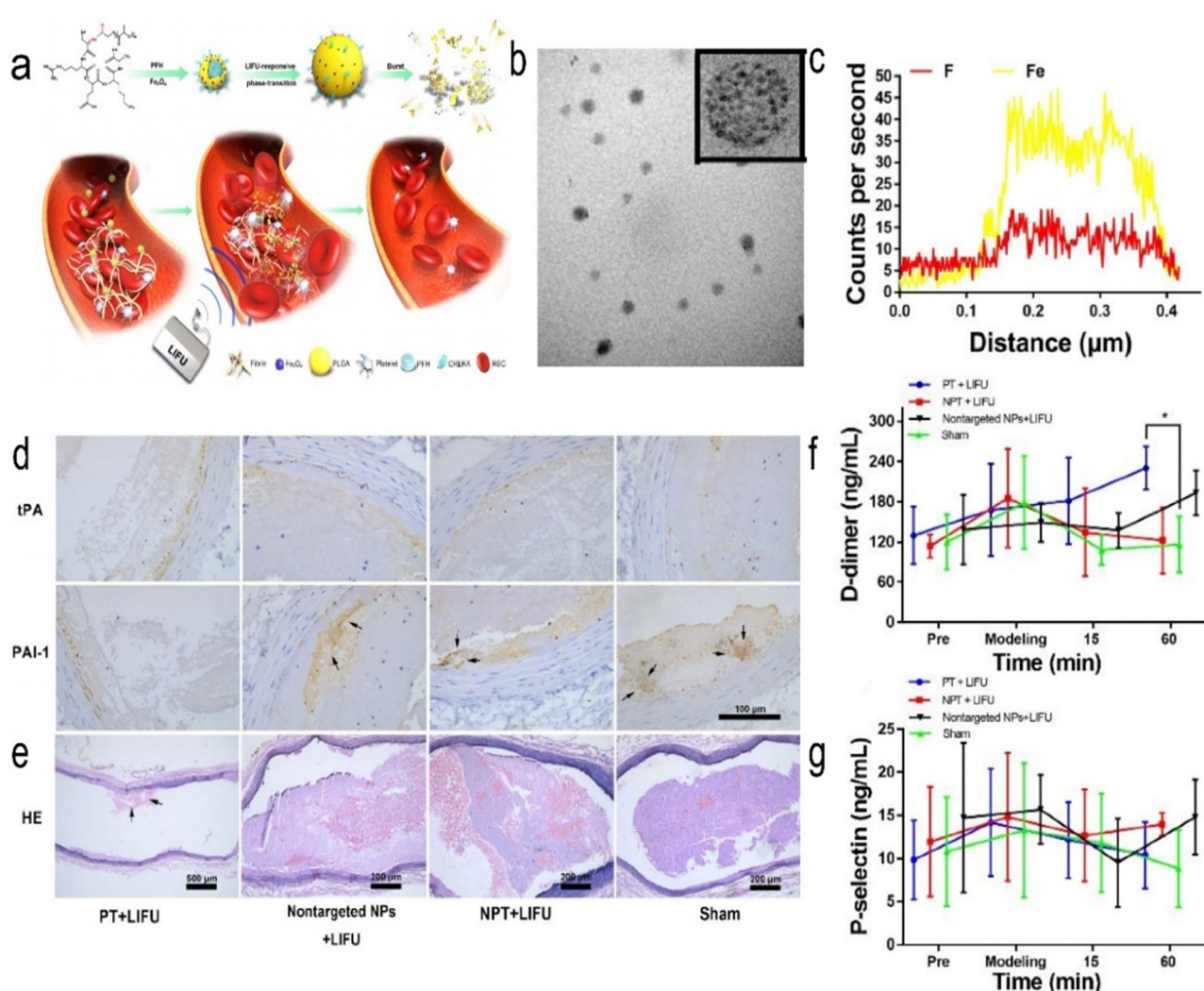


Fig. 3 (a) Schematic representation of the PT thrombolysis process, wherein LIFU pulses are applied remotely from outside the blood vessel. (b) Representative TEM images of Fe_3O_4 -PLGA-PFH-CREKA. (c) Elemental line-scan mapping of Fe_3O_4 -PLGA-PFH-CREKA NPs. (d) Representative immunohistochemistry images of tPA and PAI-1 expression. (e) Representative H&E staining images of long-axis abdominal aorta thrombosis in SD rats. (f) Changes in plasma D-dimer levels. (g) Changes in plasma P-selectin levels. Reprinted (adapted) with permission from ref. 61. Copyright 2019, American Chemical Society.

imaging signals, and the NPs can be loaded with rapamycin for neuroprotective effects.⁸⁸ Zhang *et al.* designed pH-sensitive NPs loaded with betulinic acid (BA), a natural antioxidant component.⁸⁹ NPs that combine multiple therapeutic components have also been developed. Mei *et al.* designed pH-sensitive t-PA-coated anti-oxidation self-assembled polyion-complex NPs (t-PA@iRNP). It targets ischaemic tissue and releases thrombolytic drugs and antioxidants.⁶³ Brain tissue can be protected from further damage by blood flow recirculation therapy and neuroprotective therapy, but due to the limited regenerative ability of brain tissue itself, necrotic brain tissue cannot be completely regenerated.⁹⁰ Therefore, exogenous treatment will be needed. Neural stem cells (NSCs) can regenerate and differentiate and have great potential in the treatment of IS, but their efficacy is limited in the harsh ischaemic microenvironment rich in reactive oxygen species (ROS).⁶⁵ Yang *et al.* developed a Ca-MOF@miR-124 nanoparticle, a pH-responsive nanoparticle that encounters the low pH of neural stem

cell lysozyme and releases miR-124, a miRNA that promotes neural stem cells to differentiate into mature neurons (Fig. 5).⁶⁴ It prevents the rapid degradation of miR-124 during systemic administration and increases the internalization of miR-124. The NPs were found to enhance the efficacy of NSCs in the treatment of IS, reducing ischaemic infarct size to almost normal levels by day 7.

However, due to the high complexity of biological systems, these methods suffer from off-target effects. To overcome these barriers, more stimulus response platforms can be designed to identify multiple IS characteristics and relieve off-target effects. In addition, the combination of passive targeting with active targeting would have additional advantages during drug delivery.

5.3 ROS-responsive NPs

When IS occurs, ROS in brain tissue are upregulated,⁹¹ and during ischaemia-reperfusion, ROS are explosively released,⁹² further damaging pathological tissue. Therefore, the use of



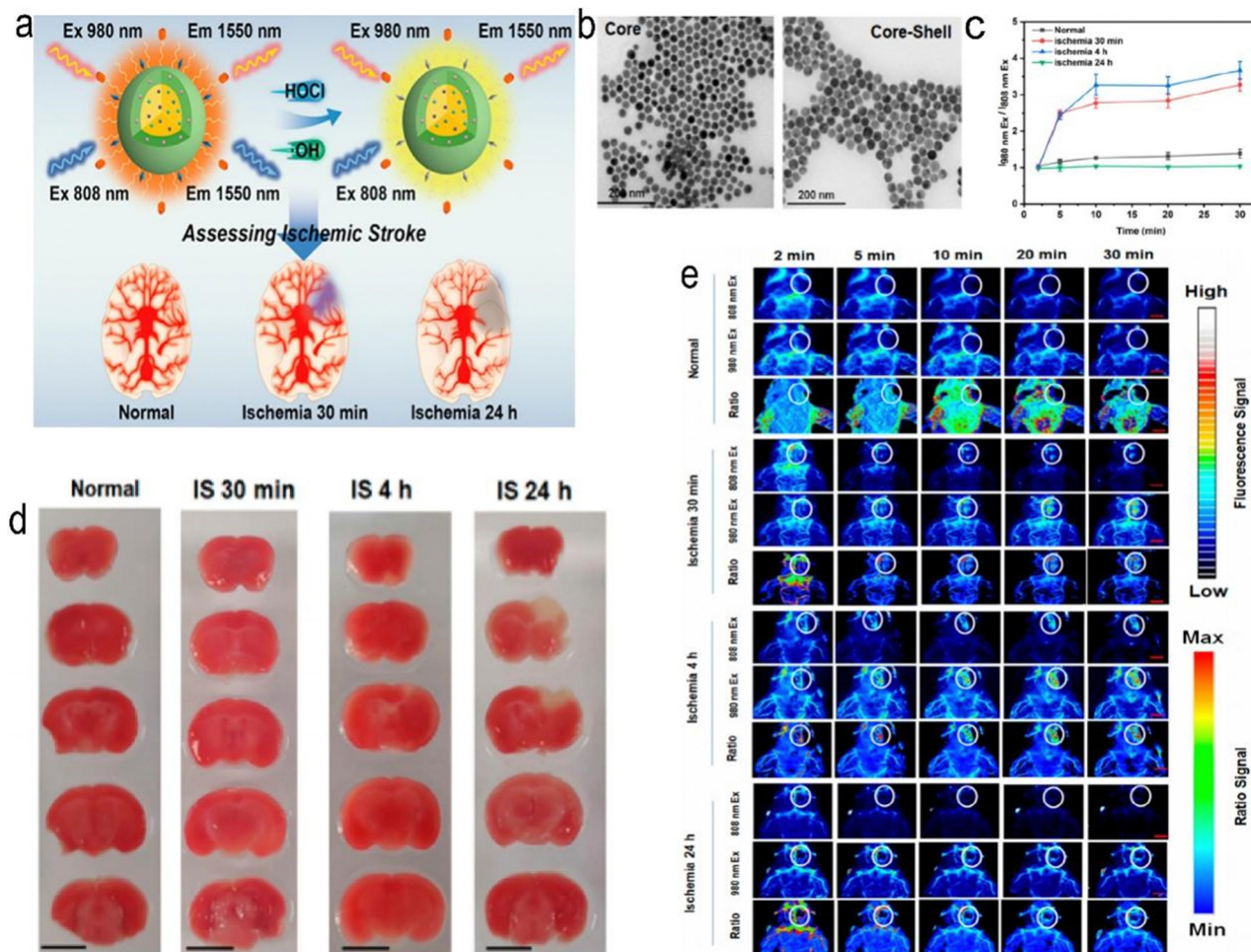


Fig. 4 (a) Schematic representation of ratiometric NIR-II luminescent nanoprobe for the treatment and assessment of IS. (b) TEM images of core (NaYbF₄:5%Er,5%Ce) and core-shell structured (NaYbF₄:5%Er,5%Ce@NaYF₄:20%Nd) LnNPs. (c) Ratio value at the lesion site for normal mice and mice with IS. (d) 2,3,5-Triphenyl tetrazolium hydrochloride (TTC) staining results for normal mice and mice with cerebral ischaemia at different times. (e) *In vivo* NIR-II luminescence imaging of normal mice and mice with cerebral ischaemia. Reprinted (adapted) with permission from ref. 62. Copyright 2021, American Chemical Society.

antioxidant drugs is necessary,^{8,93} and ROS can also be the target of targeted NPs, which have great application potential.^{94,95}

Mitochondrial volume accounts for 25% of nerve cell volume, and mitochondrial dysfunction plays a central role in IS.⁹⁶ The brain is particularly vulnerable to ROS attacks⁹⁷ because the brain is a highly oxygen-consuming organ (accounting for 20% of total body consumption), but its protective antioxidant mechanism is relatively weak.⁹⁸ Studies have shown that increased levels of oxidative stress occur in the early stage of IS and are associated with subsequent brain injury.^{99,100} Therefore, oxidative stress levels can reflect the severity of IS. Lv *et al.* developed bioengineered and ROS-responsive nanocarriers for the targeted delivery and release of the stroke-specific neuroprotective agent NR2B9C to combat ischaemic brain injury (Fig. 6).⁴² Boroester is a smart ROS-responsive biomaterial that reacts with the hydroxyl group of dextran, a glucose polymer with good water solubility and biocompatibility, and self-assembles into nanoparticles. This nanoparticle encapsulates NR2B9C, a neuroprotective agent, and forms the “core” of SHp-RBC-NP.¹⁰¹

The erythrocyte membrane has the characteristics of ultra-high biocompatibility, immune evasion ability and long blood retention time. In the erythrocyte membrane, a stroke-homing peptide (SHp, CLEVSRKNC) has been shown to selectively target brain ischaemic sites and can be colocalized in some apoptotic neurons in the penumbra area of ischaemic brain tissue to form the shell of SHp-RBC-NPs.¹⁰² When these NPs are fabricated to target ischaemic brain tissue, these NPs can control the release of NR2B9C from ischaemic neurons triggered by high intracellular ROS. A rat model of middle cerebral artery occlusion (MCAO) was established. The results of *in vitro* experiments showed that SHp-RBC-NPs antagonized glutamate-induced cytotoxicity in PC-12 cells. The same results were obtained *in vivo*, in which the retention time of NR2B9C in the systemic circulation was increased, which enhanced the active targeting of the ischaemic region in MCAO rats. The results showed that the NPs significantly reduced infarct size and improved neurological scores. Meanwhile, the NPs also showed good biocompatibility in the safety evaluation. Endogenous NSCs



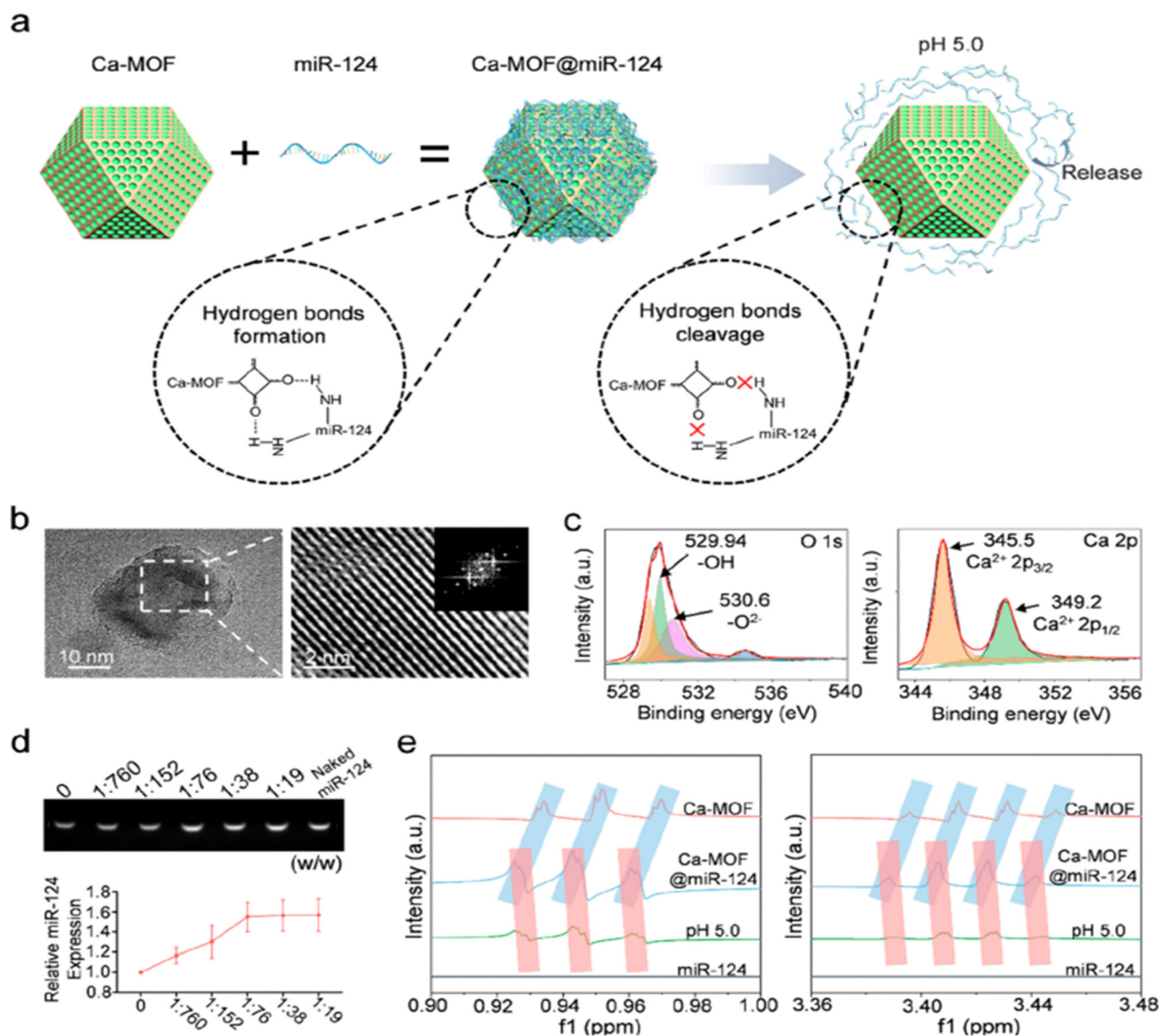


Fig. 5 Design and characterization of Ca-MOF@miR-124 NPs. (a) Diagram of the effective loading of miR-124 onto the surface of Ca-MOF. (b) TEM image and HRTEM image of the Ca-MOF NPs in the supernatant after ultrasonication. (c) XPS analysis of Ca-MOF showing its elemental composition. (d) Agarose gel electrophoresis analysis of miR-124 in Ca-MOF@miR-124 NPs. (e) ¹H NMR spectra of miR-124, Ca-MOF NPs, and Ca-MOF@miR-124 NPs. Reprinted (adapted) with permission from ref. 64. Copyright 2022, American Chemical Society.

have the potential to differentiate into other neural cells.¹⁰³ Endogenous neural stem cells (NSCs) can migrate to the lesion site after IS.^{104,105} It has functions such as cell replacement, neurotrophic effects and immune regulation.¹⁰⁶ Jiang *et al.* developed a ROS-responsive charge-reversal poly[[2-acryloyl] ethyl (p-boronic acid benzyl) diethylammonium bromide] (B-PDEA) nanoparticle, which transfected brain-derived neurotrophic factor (BDNF) into endogenous NSCs, thereby sustaining the expression of BDNF and providing neuroprotective effects.⁶⁵ Jin *et al.* synthesized ROS-responsive GA-conjugated diethylaminoethylene (DEAE)-dextran NPs (DGA) to inhibit microglial polarization manipulated by high mobility group Box 1 (HMGB1) to improve the efficacy of cerebral ischaemia therapy.⁶⁶ Activated platelets are the building blocks of thrombosis.^{107,108} Thrombosis is often accompanied by

elevated ROS.¹⁰⁹ The increase in ROS can be used as a target for the development of ROS-responsive NPs, and scavenging ROS is a potential therapeutic tool for thrombus removal.^{110,111} Wang *et al.*⁶⁷ developed platelet-targeted theranostic NPs (CyBA/PFM NPs). Amphiphilic phenylboronated fucoidan/maltodextrin (PHB-Fuco/Malto) polymers were synthesized by introducing hydrophobic phenylboronic branched chains into hydrophilic fucoidan/maltodextrin hybrid polysaccharides. The NPs were then self-assembled with the H₂O₂-sensitive “switching signal” near-infrared (NIR, 650–900 nm) probe CyBA. The NPs could remove ROS, remove clots, turn on the acousto-optic signal by short laser pulses with a length of several nanoseconds,¹¹² and then use multispectral photoacoustic tomography (MSOT) to detect vessels at a depth of 1–5 cm in a noninvasive manner with high resolution and high contrast.^{112–114}



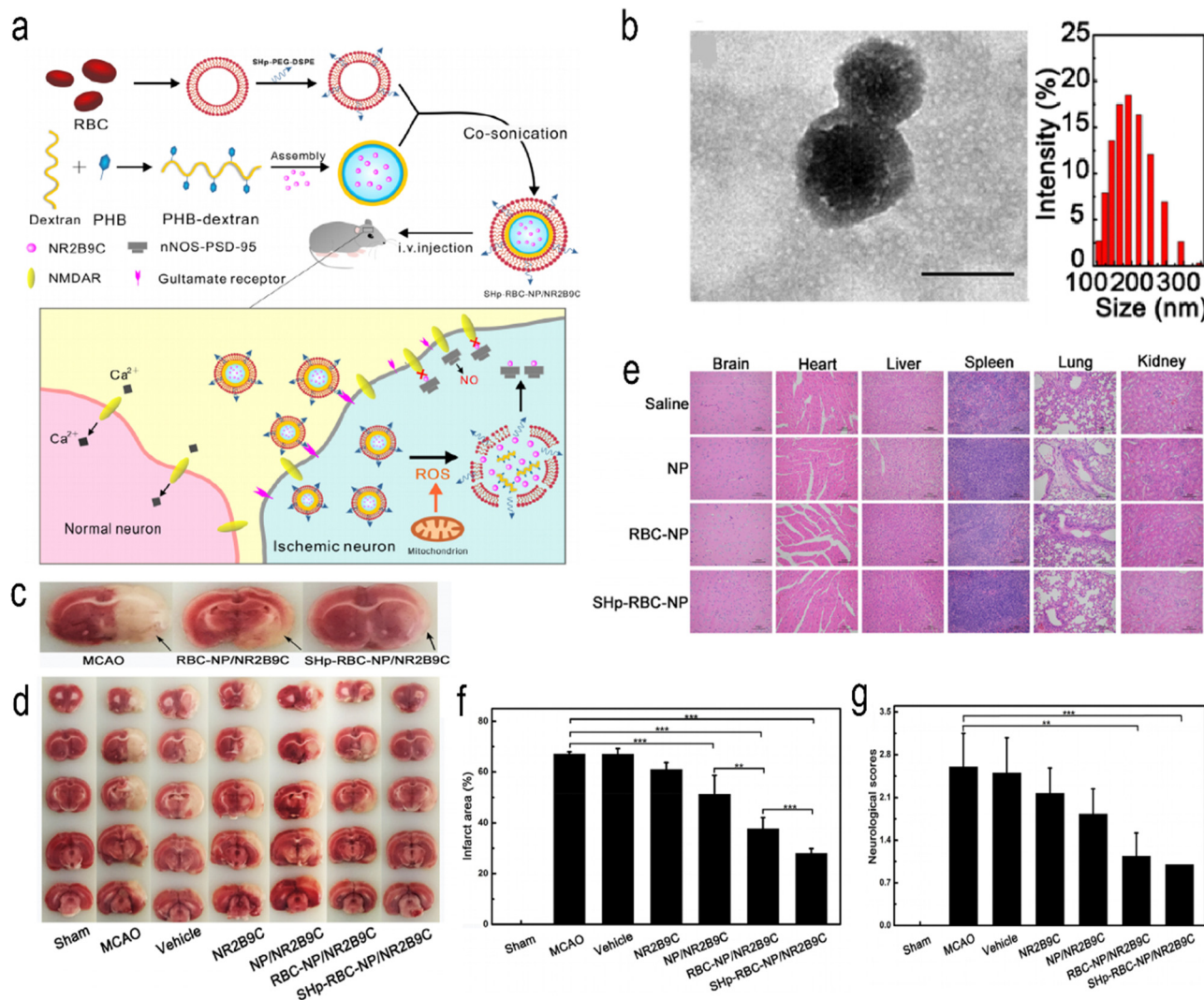


Fig. 6 (a) Schematic design of SHp-RBC-NP/NR2B9C. (b) TEM images and hydrodynamic size distribution of RBC-coated NPs. (c) Representative tissue slices showing that the RBC-NP/NR2B9C and SHp-RBC-NP/NR2B9C groups had significantly reduced infarct volumes. (d) Representative TTC-stained brain sections. (e) Histochemistry analysis of brain, heart, liver, spleen, lung, and kidney tissue sections stained with haematoxylin–eosin. (f) Quantification of brain infarct volume at 24 h after MCAO in rats. (g) Neurological scores of rats after cerebral ischaemia. Reprinted (adapted) with permission from ref. 42. Copyright 2018, American Chemical Society.

The neuroprotective mechanisms of these antioxidants need further understanding. In addition, mitochondria are the key organelles for ROS production, and a better understanding of the mechanism of ROS production and more precise targeting of mitochondria may yield just the right therapeutic effect. In addition, the production and concentration of ROS *in vivo* are also dynamically changing. It is also a challenge to distinguish between normal levels of ROS and pathological sites. Considering clinical translation, biocompatibility, nontoxicity, and immunogenicity should all be considered.

5.4 Enzyme-responsive NPs

Guo *et al.* reported brain-targeting AMD3100-conjugated, size shrinkable NPs (ASNPs) that respond to proteases to improve stroke treatment.⁶⁸ The NPs respond to thrombin or matrix metalloproteinase 9 (MMP-9). Brain targeting is mediated by the interaction of AMD3100 with CXCR4, which is abundant in

ischaemic brain tissue. ASNPs significantly improved the efficiency of gliburide penetrating cerebral ischaemia and reduced the side effects of systemic gliburide administration (Fig. 7). The experimental results show that the NPs can effectively penetrate the BBB and have strong specificity for ischaemic tissue. At the same time, it has high safety and low toxicity. To achieve clinical translation, higher biosafety and targeting are necessary. Additionally, further clarification of the biological role of MMPs *in vivo* is the foundation of designing efficient targeted nanoparticles.

6. Targeted NPs to overcome the blood–brain barrier

The BBB has numerous functions and important roles.^{115,116} The BBB is mainly composed of a physical barrier and a selective



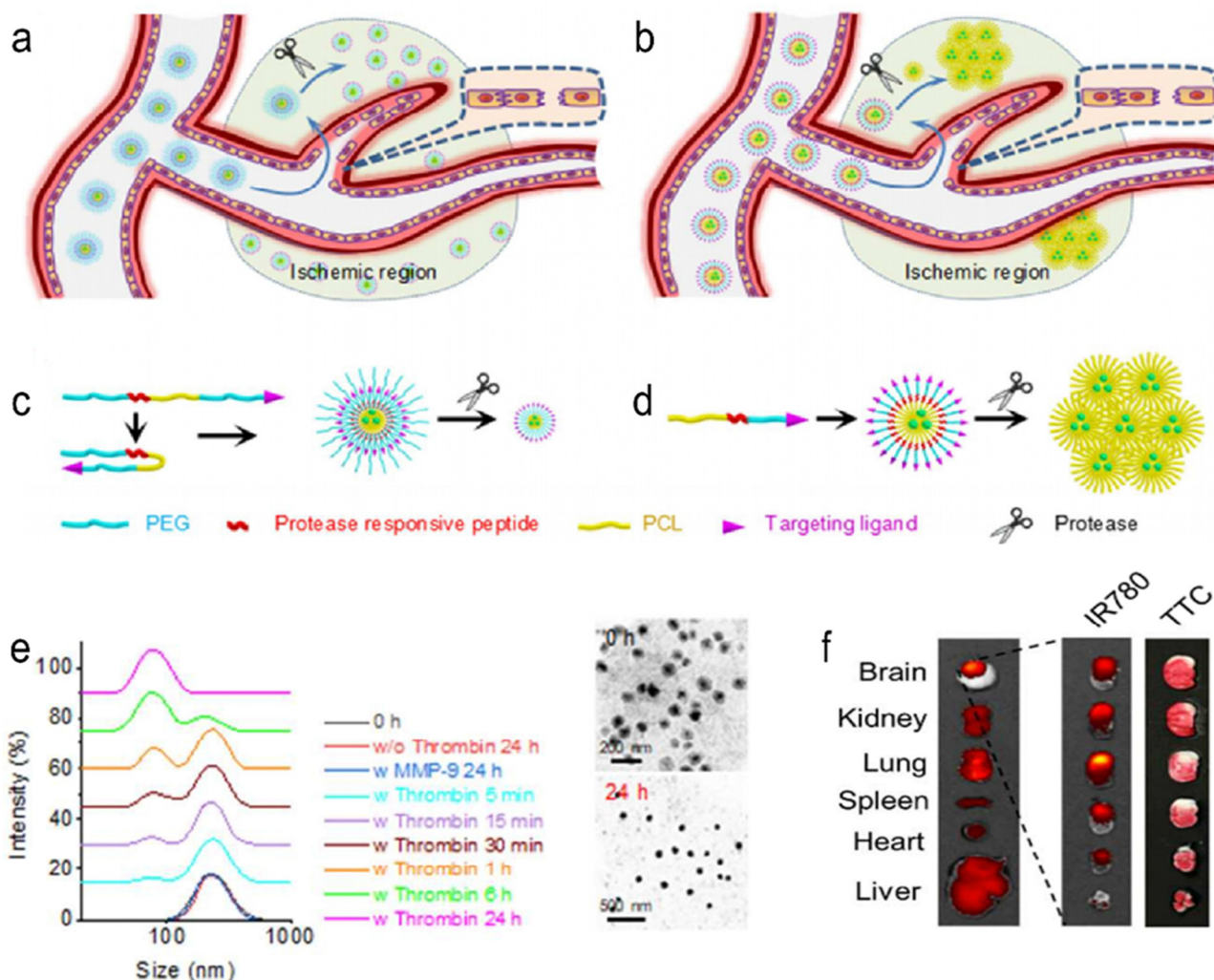


Fig. 7 Schematic diagrams of shrinkable (a) and (c) and expandable (b) and (d) micellar NPs in response to proteases enriched in the ischaemic microenvironment. (e) Dynamic light scattering (DLS) (left) and TEM (right) analyses of PEGoPCLoToPEG NPs in PBS with or without thrombin/MMP-9. (f) Representative images of brain slices with TTC staining (left) and fluorescence imaging (right). Reprinted (adapted) with permission from ref. 68. Copyright 2018, American Chemical Society.

metabolic drive barrier. The physical barrier consists of infiltrated brain microvascular endothelial cells and the tight junctions between them. In addition, tight junction proteins and adherens junction proteins expressed by brain microvascular cells contribute to high transendothelial electrical resistance. These structures limit immune surveillance cells (macrophages), transport of xenobiotic and endogenous compounds, and paracellular access of water and solutes. The selective metabolic drive barrier primarily reflects the expression and function of several receptors, ion channels, and inflow/outflow transporters that are prominently expressed at the BBB.¹¹⁷ This is also an important reason why it is difficult to translate central nervous system treatment into clinical practice. Although there is a brief opening of the BBB after IS, it is not enough to allow drugs to enter the brain tissue at an effective therapeutic concentration.¹¹⁸ Most neuroprotective drugs do not cross the BBB.^{119,120} Traditional methods to overcome the BBB include invasive drug injection,¹²¹ which increases the chance of drugs crossing the BBB by

improving the permeability of the local BBB and the drug residence time. However, there is a risk of causing brain tissue damage. Intranasal drug administration is also an effective way to bypass the BBB. However, studies have shown that this method of delivery is inefficient.^{122,123} Mechanisms for non-invasive crossing of the BBB include passive diffusion, vector-mediated transport, and endocytic/transcellular pathways.¹²⁴ Physical barriers restrict the access of hydrophilic substances and macromolecules to the BBB. Selective metabolic drive barriers actively expel certain foreign molecules from the brain.¹²⁵ Endocytic/transcellular actions allow internalization, sorting, and transport of many plasma macromolecules.¹²⁶ Electrostatic adsorption and receptor mediation are involved in this process. Targeted NPs can enter cells through tight junctions between endothelial cells in the BBB,¹²⁷ through endocytosis, or through receptor-mediated entry. Currently, the most effective strategy for crossing the BBB is to bind to receptors on the BBB by promoting receptor transport. Shen *et al.* developed a



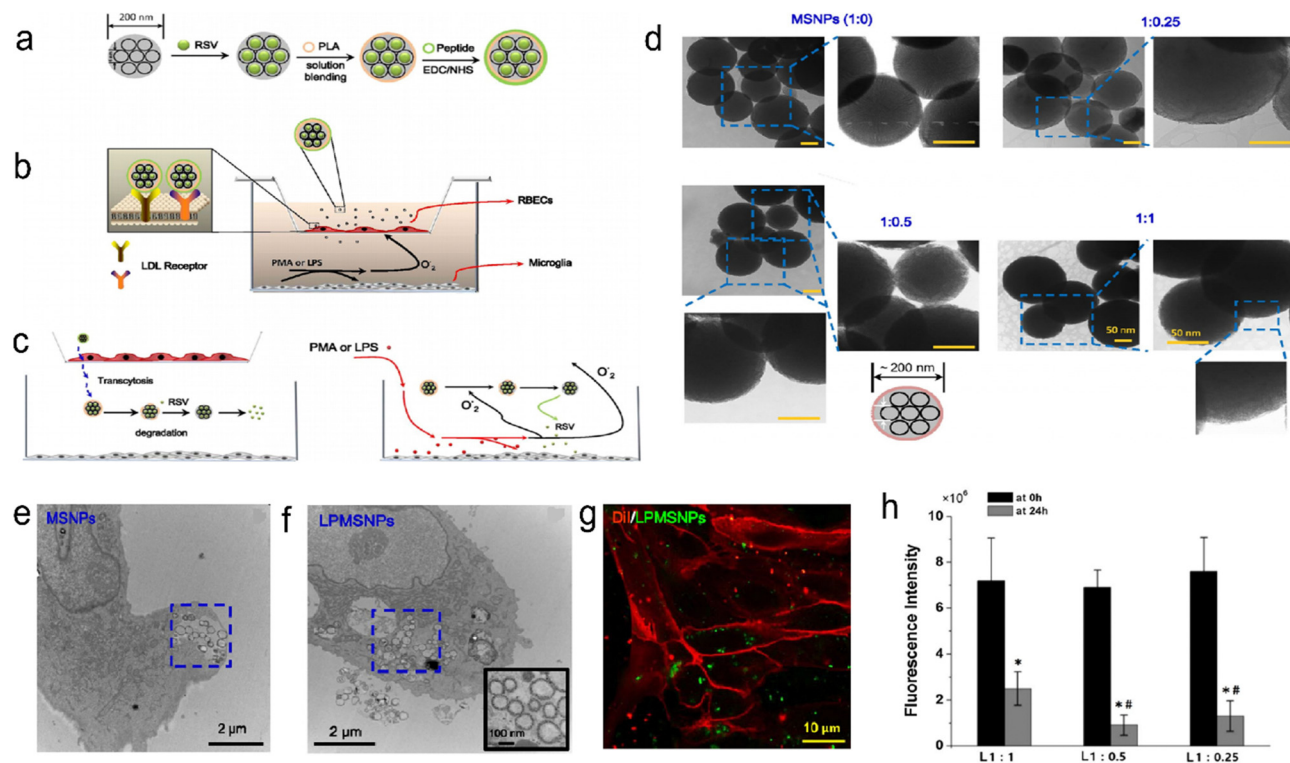


Fig. 8 Schematic of the MSNP delivery system. (a) Design of RSV-loaded MSNPs with a peptide-bound PLA coating. (b) An *in vitro* BBB model with RBECs cultured on semipermeable membranes of a Transwell chamber. (c) PMA- or LPS-stimulated microglia produce superoxide or nitric oxide. (d) TEM images of PLA-coated MSNPs with different mass ratios. (e) TEM image of MSNPs internalized by an RBEC. (f) TEM image of LDL peptide-decorated PMSNPs internalized by an RBEC. (g) Fluorescence images showing RBECs cultured with LPMSNPs. (h) The fluorescence intensity of FTIC-labelled PMSNPs in the upper Transwell chamber. Reprinted (adapted) with permission from ref. 28. Copyright 2018, The Author(s).

nanoparticle that binds to low-density lipoprotein receptors (LDLR), a resveratrol (RSV) delivery vector based on polylactic acid (PLA)-coated mesoporous silica NPs (MSNPs) (Fig. 8). In an *in vitro* BBB model of rat brain microvascular endothelial cells (RBECs) cocultured with microglia established in a Transwell chamber, the migration of NPs through the monomolecular layer of rat brain microvascular endothelial cells (RBECs) was significantly enhanced by coupling with LDLR.²⁸ ROS production leads to the aggregation of inflammatory cells at the lesion site,¹²⁸ which provides opportunities for therapeutic macromolecules that cannot cross the BBB.¹²⁹ Zhang *et al.* developed a cl PGP-PEG-DGL/CAT-Aco system. that binds neutrophils, crosses the BBB with neutrophils, reaches the site of injury and is finally released to play a role in antioxidant therapy.²³

7. Conclusions and outlook

Ischaemic stroke (IS) is a serious threat to human health with high morbidity, mortality, and disability rates. Although reperfusion therapy has been widely used and proven effective, most patients are still left with long-term neurological impairment due to the narrow treatment time window and ischaemia-reperfusion injury. Although many drugs have been developed to treat ischaemic stroke, they are not effective because they do not effectively penetrate the BBB and target ischaemic tissue in

the brain. New treatment strategies need to be developed. Targeted NPs show advantages in penetrating the BBB and targeting diseased tissues by changing their composition and structure. This paper reviews the therapeutic strategies and advances of using targeted NPs in the treatment of IS. Although great progress has been made, there are still many challenges. First, the targeted NPs use an endogenous substance at the site of the lesion as a target, but the concentration of the substance needs to be high enough to distinguish the lesion from normal tissue. In addition, due to the complex pathological mechanism, the endogenous substance concentration as the target often has temporal and spatial dynamic changes. Therefore, the developed targeted NPs should also have corresponding mechanisms. Second, targeted NPs will still miss the target. Therefore, active targeting, passive targeting and multiple targeting are often combined to improve targeting, but this also increases the difficulty of manufacturing NPs. Third, we should also consider the biocompatibility and degradability of this exogenous synthetic material. Fourth, the implementation of clinical transformation, including biological stability, effectiveness and safety evaluation, mass production, consistency, evaluation standards, storage stability, *etc.*^{25,130} Finally, the pathophysiological mechanism of IS needs further investigation, which is the basis for our development of responsive nanoparticle targets. Although many challenges remain, targeted NPs have proven to be effective in the prevention,



detection, and treatment of IS and show great potential. With advances in nanotechnology, more complex processes can be applied to the preparation of NPs, and with advances in medicine, the understanding of the pathological mechanism of IS is deepened. More NPs with precise targeting ability, multiple targeting, high permeability to the BBB, high bioavailability, histocompatibility, and low toxicity will be developed. Targeted NPs are expected to become an ideal drug for the treatment of IS with broad prospects. In this review, we summarize the role of targeting NPs in the prevention, detection, and treatment of IS, providing innovative insights and clues for future developments.

Conflicts of interest

The authors declare that they have no known competing financial interests or personal relationships that could have appeared to influence the work reported in this paper.

Acknowledgements

This work was financially supported by National Natural Science Foundation of China (22372001), the Key Research Project of the Natural Science Foundation of Anhui Provincial Universities (KJ2023AH050997), the Anhui Provincial Health Commission (AHWJ2022b021, GCCRC2022019), Anhui Provincial Natural Science Foundation (2308085MH259), Natural Science Research Project of Anhui Educational Committee (2022AH040169, 2022AH051219, 2023AH051776), Yijishan Hospital Talent Special Research Fund (YR20220204), Science and Technology Project of Wuhu City (2022jc63), Open Project of Key Laboratory of Noncoding RNA Transformation Research of Anhui Higher Education Institution (RNA202201), Starting Fund for Scientific Research of High-Level Talents, Anhui Agricultural University (rc382108), Clinical Medical Research Transformation Project of Anhui Province (202304295107020002) and Research on Active Biomacromolecules at the School Level Open Project of Anhui Provincial Key Laboratory (LAB202203).

References

- C. W. Tsao, A. W. Aday, Z. I. Almarzooq, A. Alonso, A. Z. Beaton, M. S. Bittencourt, A. K. Boehme, A. E. Buxton, A. P. Carson, Y. Commodore-Mensah, M. S. V. Elkind, K. R. Evenson, C. Eze-Nliam, J. F. Ferguson, G. Generoso, J. E. Ho, R. Kalani, S. S. Khan, B. M. Kissela, K. L. Knutson, D. A. Levine, T. T. Lewis, J. Liu, M. S. Loop, J. Ma, M. E. Mussolino, S. D. Navaneethan, A. M. Perak, R. Poudel, M. Rezk-Hanna, G. A. Roth, E. B. Schroeder, S. H. Shah, E. L. Thacker, L. B. VanWagner, S. S. Virani, J. H. Voeks, N. Y. Wang, K. Yaffe and S. S. Martin, *Circulation*, 2022, **145**, e153–e639.
- Z. Wang, S. Hu, S. Sang, L. Luo and C. Yu, *Stroke*, 2017, **48**, 271–275.
- K. L. Furie and M. V. Jayaraman, *Stroke*, 2018, **49**, 509–510.
- P. Gervois, E. Wolfs, J. Ratajczak, Y. Dillen, T. Vangansewinkel, P. Hilken, A. Bronckaers, I. Lambrechts and T. Struys, *Med. Res. Rev.*, 2016, **36**, 1080–1126.
- S. S. Virani, A. Alonso, E. J. Benjamin, M. S. Bittencourt, C. W. Callaway, A. P. Carson, A. M. Chamberlain, A. R. Chang, S. Cheng, F. N. Delling, L. Djousse, M. S. V. Elkind, J. F. Ferguson, M. Fornage, S. S. Khan, B. M. Kissela, K. L. Knutson, T. W. Kwan, D. T. Lackland, T. T. Lewis, J. H. Lichtman, C. T. Longenecker, M. S. Loop, P. L. Lutsey, S. S. Martin, K. Matsushita, A. E. Moran, M. E. Mussolino, A. M. Perak, W. D. Rosamond, G. A. Roth, U. K. A. Sampson, G. M. Satou, E. B. Schroeder, S. H. Shah, C. M. Shay, N. L. Spartano, A. Stokes, D. L. Tirschwell, L. B. VanWagner and C. W. Tsao, *Circulation*, 2020, **141**, e139–e596.
- S. J. Mendelson and S. Prabhakaran, *JAMA*, 2021, **325**, 1088–1098.
- J. Castillo, M. I. Loza, D. Mirelman, J. Brea, M. Blanco, T. Sobrino and F. Campos, *J. Cereb. Blood Flow Metab.*, 2015, **36**, 292–301.
- A. Chamorro, U. Dirnagl, X. Urra and A. M. Planas, *Lancet Neurol.*, 2016, **15**, 869–881.
- C. Iadecola and J. Anrather, *Nat. Med.*, 2011, **17**, 796–808.
- S. Parvez, M. Kaushik, M. Ali, M. M. Alam, J. Ali, H. Tabassum and P. Kaushik, *Theranostics*, 2022, **12**, 689–719.
- G. A. Donnan, S. M. Davis, M. W. Parsons, H. Ma, H. M. Dewey and D. W. Howells, *Nat. Rev. Neurol.*, 2011, **7**, 400–409.
- L. H. Schwamm, S. F. Ali, M. J. Reeves, E. E. Smith, J. L. Saver, S. Messe, D. L. Bhatt, M. V. Grau-Sepulveda, E. D. Peterson and G. C. Fonarow, *Circ.: Cardiovasc. Qual. Outcomes*, 2013, **6**, 543–549.
- I. Gravanis and S. E. Tsirka, *Expert Opin. Ther. Targets*, 2008, **12**, 159–170.
- B. Frank, J. C. Grotta, A. V. Alexandrov, E. Bluhmki, P. Lyden, A. Meretoja, N. K. Mishra, A. Shuaib, N. G. Wahlgren, C. Weimar and K. R. Lees, *Stroke*, 2013, **44**, 727–733.
- W. Hacke, G. Donnan, C. Fieschi, M. Kaste, R. von Kummer, J. P. Broderick, T. Brott, M. Frankel, J. C. Grotta, E. C. Haley, Jr., T. Kwiatkowski, S. R. Levine, C. Lewandowski, M. Lu, P. Lyden, J. R. Marler, S. Patel, B. C. Tilley, G. Albers, E. Bluhmki, M. Wilhelm and S. Hamilton, *Lancet*, 2004, **363**, 768–774.
- S. Cadenas, *Free Radic. Biol. Med.*, 2018, **117**, 76–89.
- C. L. Allen and U. Bayraktutan, *Int. J. Stroke*, 2009, **4**, 461–470.
- C. G. Kevil, T. Oshima, B. Alexander, L. L. Coe and J. S. Alexander, *Am. J. Physiol.: Cell Physiol.*, 2000, **279**, C21–C30.
- P. J. Kelly, J. D. Morrow, M. Ning, W. Koroshetz, E. H. Lo, E. Terry, G. L. Milne, J. Hubbard, H. Lee, E. Stevenson, M. Lederer and K. L. Furie, *Stroke*, 2008, **39**, 100–104.
- H. K. Eltzschig and T. Eckle, *Nat. Med.*, 2011, **17**, 1391–1401.
- V. E. O'Collins, M. R. Macleod, G. A. Donnan, L. L. Horky, B. H. van der Worp and D. W. Howells, *Ann. Neurol.*, 2006, **59**, 467–477.



- 22 M. V. Sofroniew and H. V. Vinters, *Acta Neuropathol.*, 2010, **119**, 7–35.
- 23 C. Zhang, C. L. Ling, L. Pang, Q. Wang, J. X. Liu, B. S. Wang, J. M. Liang, Y. Z. Guo, J. Qin and J. X. Wang, *Theranostics*, 2017, **7**, 3260–3275.
- 24 H. Wu, T. Zhang, N. Li and J. Gao, *J. Controlled Release*, 2023, **360**, 169–184.
- 25 B. Choi, W. Park, S.-B. Park, W.-K. Rhim and D. K. Han, *Methods*, 2020, **177**, 2–14.
- 26 S. Zhang, Y. Zhou, R. Li, Z. Chen and X. Fan, *J. Controlled Release*, 2022, **344**, 173–201.
- 27 S. Mehta, V. Bongcaron, T. K. Nguyen, Y. Jirwanka, A. Maluenda, A. P. G. Walsh, J. Palasubramaniam, M. D. Hulett, R. Srivastava, A. Bobik, X. Wang and K. Peter, *Small*, 2022, **18**, e2200967.
- 28 Y. Shen, B. Cao, N. R. Snyder, K. M. Woepfel, J. R. Eles and X. T. Cui, *J. Nanobiotechnol.*, 2018, **16**, 13.
- 29 B. C. V. Campbell, D. A. De Silva, M. R. Macleod, S. B. Coutts, L. H. Schwamm, S. M. Davis and G. A. Donnan, *Nat. Rev. Dis. Primers*, 2019, **5**, 70.
- 30 J. L. Mega and T. Simon, *Lancet*, 2015, **386**, 281–291.
- 31 X. Wang, M. Ouyang, J. Yang, L. Song, M. Yang and C. S. Anderson, *Cochrane Database Syst. Rev.*, 2021, **10**, CD000024.
- 32 P. A. Sandercock, C. Counsell and E. J. Kane, *Cochrane Database Syst. Rev.*, 2015, **2015**, CD000024.
- 33 J. Zhu, M. Ma, Y. Guo, M. Zhou, J. Guo and L. He, *BMC Neurol.*, 2018, **18**, 194.
- 34 K. H. Choi, J. H. Kim, C. Lee, J. M. Kim, K. W. Kang, J. T. Kim, S. M. Choi, M. S. Park and K. H. Cho, *Stroke*, 2020, **51**, 3514–3522.
- 35 L. Chen, S. Cao and J. Yang, *Neurol. Res.*, 2018, **40**, 862–867.
- 36 P. Tanswell, N. Modi, D. Combs and T. Danays, *Clin. Pharmacokinet.*, 2002, **41**, 1229–1245.
- 37 J. Horn, R. J. de Haan, M. Vermeulen, P. G. Luiten and M. Limburg, *Stroke*, 2001, **32**, 2433–2438.
- 38 H. Zheng, Y. Wang, A. Wang, H. Li, D. Wang, X. Zhao, P. Wang, H. Shen, L. Zuo, Y. Pan, Z. Li, X. Meng, X. Wang, W. Shi, Y. Ju, L. Liu, K. Dong, C. Wang, R. Sui, R. Xue, X. Pan, X. Niu, B. Luo, Y. Sui, H. Wang, T. Feng and Y. Wang, *Sci. Bull.*, 2019, **64**, 101–107.
- 39 T. Wada, H. Yasunaga, R. Inokuchi, H. Horiguchi, K. Fushimi, T. Matsubara, S. Nakajima and N. Yahagi, *J. Neurol. Sci.*, 2014, **345**, 106–111.
- 40 M. Trotman, P. Vermehren, C. L. Gibson and R. Fern, *J. Cereb. Blood Flow Metab.*, 2015, **35**, 230–239.
- 41 S. M. Seyedasadat and D. F. Kallmes, *Rev. Neurosci.*, 2019, **30**, 203–220.
- 42 W. Lv, J. Xu, X. Wang, X. Li, Q. Xu and H. Xin, *ACS Nano*, 2018, **12**, 5417–5426.
- 43 T. Huang, N. Li and J. Gao, *Asian J. Pharm. Sci.*, 2019, **14**, 233–247.
- 44 N. Mackman, *Nature*, 2008, **451**, 914–918.
- 45 B. C. V. Campbell, P. J. Mitchell, L. Churilov, N. Yassi, T. J. Kleinig, R. J. Dowling, B. Yan, S. J. Bush, H. M. Dewey, V. Thijs, R. Scroop, M. Simpson, M. Brooks, H. Asadi, T. Y. Wu, D. G. Shah, T. Wijeratne, T. Ang, F. Miteff, C. R. Levi, E. Rodrigues, H. Zhao, P. Salvaris, C. Garcia-Esperon, P. Bailey, H. Rice, L. de Villiers, H. Brown, K. Redmond, D. Leggett, J. N. Fink, W. Collecutt, A. A. Wong, C. Muller, A. Coulthard, K. Mitchell, J. Clouston, K. Mahady, D. Field, H. Ma, T. G. Phan, W. Chong, R. V. Chandra, L. A. Slater, M. Krause, T. J. Harrington, K. C. Faulder, B. S. Steinfors, C. F. Bladin, G. Sharma, P. M. Desmond, M. W. Parsons, G. A. Donnan and S. M. Davis, *N. Engl. J. Med.*, 2018, **378**, 1573–1582.
- 46 R. L. Medcalf, *Br. J. Pharmacol.*, 2012, **165**, 75–89.
- 47 S. Amemiya, T. Kamiya, C. Nito, T. Inaba, K. Kato, M. Ueda, K. Shimazaki and Y. Katayama, *Eur. J. Pharmacol.*, 2005, **516**, 125–130.
- 48 G. Edaravone Acute Infarction Study, *Cerebrovasc. Dis.*, 2003, **15**, 222–229.
- 49 Y. Fu, N. Zhang, L. Ren, Y. Yan, N. Sun, Y. J. Li, W. Han, R. Xue, Q. Liu, J. Hao, C. Yu and F. D. Shi, *Proc. Natl. Acad. Sci. U. S. A.*, 2014, **111**, 18315–18320.
- 50 J. Huang, T. F. Choudhri, C. J. Winfree, R. A. McTaggart, S. Kiss, J. Mocco, L. J. Kim, T. S. Protopsaltis, Y. Zhang, D. J. Pinsky and E. S. Connolly, Jr., *Stroke*, 2000, **31**, 3047–3053.
- 51 J. Xiang, R. Zhao, B. Wang, X. Sun, X. Guo, S. Tan and W. Liu, *Front. Oncol.*, 2021, **11**, 758143.
- 52 R. Bendayan, G. Lee and M. Bendayan, *Microsc. Res. Tech.*, 2002, **57**, 365–380.
- 53 J. Zhu, W. Chen, Y. Sun, X. Huang, R. Chu, R. Wang, D. Zhou and S. Ye, *Mater. Adv.*, 2022, **3**, 7687–7708.
- 54 J. Zhu, R. Hou, M. Liu, L. Wang, W. Chen, Y. Sun, W. Wei and S. Ye, *Mater. Today Sustainability*, 2022, **18**, 100125.
- 55 H. L. Wong, X. Y. Wu and R. Bendayan, *Adv. Drug Delivery Rev.*, 2012, **64**, 686–700.
- 56 R. Zhong, R. Chu, J. Zhu, J. Ling, L. Zhang, Y. Zhou, M. Yin, Z. Hao, C. Liang, S. Cao, T. Xu, S. Ye and S. Fan, *Mater. Today Sustainability*, 2023, **21**, 100323.
- 57 P. M. Winter, A. M. Morawski, S. D. Caruthers, R. W. Fuhrop, H. Zhang, T. A. Williams, J. S. Allen, E. K. Lacy, J. D. Robertson, G. M. Lanza and S. A. Wickline, *Circulation*, 2003, **108**, 2270–2274.
- 58 L. O. Sillerud, Y. Yang, L. Y. Yang, K. B. Duval, J. Thompson and Y. Yang, *J. Cereb. Blood Flow Metab.*, 2020, **40**, S117–S133.
- 59 H. A. Chen, Y. H. Ma, T. Y. Hsu and J. P. Chen, *Int. J. Mol. Sci.*, 2020, **21**, 2690.
- 60 J. Hu, S. Huang, L. Zhu, W. Huang, Y. Zhao, K. Jin and Q. ZhuGe, *ACS Appl. Mater. Interfaces*, 2018, **10**, 32988–32997.
- 61 Y. Zhong, Y. Zhang, J. Xu, J. Zhou, J. Liu, M. Ye, L. Zhang, B. Qiao, Z. G. Wang, H. T. Ran and D. Guo, *ACS Nano*, 2019, **13**, 3387–3403.
- 62 M. Zhang, Z. Wang, C. Wang, Y. Wu, Z. Li and Z. Liu, *ACS Nano*, 2021, **15**, 11940–11952.
- 63 T. Mei, A. Kim, L. B. Vong, A. Marushima, S. Puentes, Y. Matsumaru, A. Matsumura and Y. Nagasaki, *Biomaterials*, 2019, **215**, 119209.



- 64 H. Yang, M. Han, J. Li, H. Ke, Y. Kong, W. Wang, L. Wang, W. Ma, J. Qiu, X. Wang, T. Xin and H. Liu, *ACS Nano*, 2022, **16**, 14503–14516.
- 65 X. C. Jiang, J. J. Xiang, H. H. Wu, T. Y. Zhang, D. P. Zhang, Q. H. Xu, X. L. Huang, X. L. Kong, J. H. Sun, Y. L. Hu, K. Li, Y. Tabata, Y. Q. Shen and J. Q. Gao, *Adv. Mater.*, 2019, **31**, e1807591.
- 66 L. Jin, Z. Zhu, L. Hong, Z. Qian, F. Wang and Z. Mao, *Bioact. Mater.*, 2023, **19**, 38–49.
- 67 Y. Wang, C. Jian, Y. Long, X. Xu, Y. Song and Z. Yin, *Acta Biomater.*, 2023, **158**, 769–781.
- 68 X. Guo, G. Deng, J. Liu, P. Zou, F. Du, F. Liu, A. T. Chen, R. Hu, M. Li, S. Zhang, Z. Tang, L. Han, J. Liu, K. N. Sheth, Q. Chen, X. Gou and J. Zhou, *ACS Nano*, 2018, **12**, 8723–8732.
- 69 L. L. Israel, A. Galstyan, E. Holler and J. Y. Ljubimova, *J. Controlled Release*, 2020, **320**, 45–62.
- 70 M. Jeon, M. V. Halbert, Z. R. Stephen and M. Zhang, *Adv. Mater.*, 2020, **33**, e1906539.
- 71 J. W. Bulte and D. L. Kraitchman, *Curr. Pharm. Biotechnol.*, 2004, **5**, 567–584.
- 72 M. Wiart, N. Davoust, J. B. Pialat, V. Desestret, S. Moucharrarie, T. H. Cho, M. Mutin, J. B. Langlois, O. Beuf, J. Honnorat, N. Nighoghossian and Y. Berthezène, *Stroke*, 2007, **38**, 131–137.
- 73 Z. W. Tay, S. Savliwala, D. W. Hensley, K. L. B. Fung, C. Colson, B. D. Fellows, X. Zhou, Q. Huynh, Y. Lu, B. Zheng, P. Chandrasekharan, S. M. Rivera-Jimenez, C. M. Rinaldi-Ramos and S. M. Conolly, *Small Methods*, 2021, **5**, e2100796.
- 74 N. Nighoghossian, M. Wiart, S. Cakmak, Y. Berthezène, L. Derex, T. H. Cho, C. Nemoz, F. Chapuis, G. L. Tisserand, J. B. Pialat, P. Trouillas, J. C. Froment and M. Hermier, *Stroke*, 2007, **38**, 303–307.
- 75 M. Li, J. Li, J. Chen, Y. Liu, X. Cheng, F. Yang and N. Gu, *ACS Nano*, 2020, **14**, 2024–2035.
- 76 Y. C. Chen, A. L. Huang, T. S. Kyaw, A. Bobik and K. Peter, *Arterioscler., Thromb., Vasc. Biol.*, 2016, **36**, e63–e72.
- 77 X. Wang and K. Peter, *Arterioscler., Thromb., Vasc. Biol.*, 2017, **37**, 1029–1040.
- 78 E. Nance, K. Timbie, G. W. Miller, J. Song, C. Louttit, A. L. Klibanov, T. Y. Shih, G. Swaminathan, R. J. Tamargo, G. F. Woodworth, J. Hanes and R. J. Price, *J. Controlled Release*, 2014, **189**, 123–132.
- 79 Y. Kung, C. Lan, M.-Y. Hsiao, M.-K. Sun, Y.-H. Hsu, A. P. H. Huang, W.-H. Liao, H.-L. Liu, C. Insera and W.-S. Chen, *Sci. Rep.*, 2018, **8**, 2218.
- 80 Y. Lampl, J. A. Zivin, M. Fisher, R. Lew, L. Welin, B. Dahlof, P. Borenstein, B. Andersson, J. Perez, C. Caparo, S. Illic and U. Oron, *Stroke*, 2007, **38**, 1843–1849.
- 81 P. A. Lapchak, J. Wei and J. A. Zivin, *Stroke*, 2004, **35**, 1985–1988.
- 82 W. Chen, R. Chu, H. Li, T. Hua, H. Chen, R. Li, D. Zhou, S. Cao, S. Ye and H. Li, *Mater. Adv.*, 2023, **4**, 2918.
- 83 J. Klohs, A. Wunder and K. Licha, *Basic Res. Cardiol.*, 2008, **103**, 144–151.
- 84 P. A. Lapchak, *Ann. Med.*, 2010, **42**, 576–586.
- 85 J. Shao, M. Abdelghani, G. Shen, S. Cao, D. S. Williams and J. C. M. van Hest, *ACS Nano*, 2018, **12**, 4877–4885.
- 86 L. H. Chang, E. Y. Chuang, T. M. Cheng, C. Lin, C. M. Shih, A. T. Wu, P. R. Jheng, H. Y. Lu, C. C. Shih and F. L. Mi, *Acta Biomater.*, 2021, **134**, 686–701.
- 87 S. Yao, C. He, P. Yuan, X. Xu, X. Zhou, L. Shen, Q. Hu, N. K. H. Slater, W. Sun, Y. Shen, H. Hu and J. Tang, *Adv. Healthcare Mater.*, 2022, e2201981.
- 88 Y. Cheng, A. Cheng, Y. Jia, L. Yang, Y. Ning, L. Xu, Y. Zhong, Z. Zhuang, J. Guan, X. Zhang, Y. Lin, T. Zhou, X. Fan, J. Li, P. Liu, G. Yan and R. Wu, *ACS Appl. Mater. Interfaces*, 2021, **13**, 56909–56922.
- 89 S. Zhang, B. Peng, Z. Chen, J. Yu, G. Deng, Y. Bao, C. Ma, F. Du, W. C. Sheu, W. T. Kimberly, J. M. Simard, D. Coman, Q. Chen, F. Hyder, J. Zhou and K. N. Sheth, *Bioact. Mater.*, 2022, **16**, 57–65.
- 90 R. Lemmens and G. K. Steinberg, *Curr. Opin. Neurol.*, 2013, **26**, 617–625.
- 91 Z. Ren, S. Sun, R. Sun, G. Cui, L. Hong, B. Rao, A. Li, Z. Yu, Q. Kan and Z. Mao, *Adv. Mater.*, 2020, **32**, e1906024.
- 92 E. T. Chouchani, V. R. Pell, E. Gaude, D. Aksentijević, S. Y. Sundier, E. L. Robb, A. Logan, S. M. Nadtochiy, E. N. J. Ord, A. C. Smith, F. Eyassu, R. Shirley, C. H. Hu, A. J. Dare, A. M. James, S. Rogatti, R. C. Hartley, S. Eaton, A. S. H. Costa, P. S. Brookes, S. M. Davidson, M. R. Duchon, K. Saeb-Parsy, M. J. Shattock, A. J. Robinson, L. M. Work, C. Frezza, T. Krieg and M. P. Murphy, *Nature*, 2014, **515**, 431–435.
- 93 M. Petro, H. Jaffer, J. Yang, S. Kabu, V. B. Morris and V. Labhassetwar, *Biomaterials*, 2016, **81**, 169–180.
- 94 T. Zhao, W. Wu, L. Sui, Q. Huang, Y. Nan, J. Liu and K. Ai, *Bioact. Mater.*, 2022, **7**, 47–72.
- 95 L. Hu, Z. Cao, L. Ma, Z. Liu, G. Liao, J. Wang, S. Shen, D. Li and X. Yang, *Biomaterials*, 2019, **223**, 119469.
- 96 N. K. Mondal, J. Behera, K. E. Kelly, A. K. George, P. K. Tyagi and N. Tyagi, *Neurochem. Int.*, 2019, **122**, 120–138.
- 97 A. Popa-Wagner, S. Mitran, S. Sivanesan, E. Chang and A. M. Buga, *Oxid. Med. Cell. Longevity*, 2013, **2013**, 963520.
- 98 W. Chen and D. Li, *Front. Chem.*, 2020, **8**, 732.
- 99 E. H. Lo, T. Dalkara and M. A. Moskowitz, *Nat. Rev. Neurosci.*, 2003, **4**, 399–415.
- 100 M. A. Moskowitz, E. H. Lo and C. Iadecola, *Neuron*, 2010, **67**, 181–198.
- 101 K. E. Broaders, S. Grandhe and J. M. J. Fréchet, *J. Am. Chem. Soc.*, 2010, **133**, 756–758.
- 102 H.-Y. Hong, J. S. Choi, Y. J. Kim, H. Y. Lee, W. Kwak, J. Yoo, J.-T. Lee, T.-H. Kwon, I.-S. Kim, H.-S. Han and B.-H. Lee, *J. Controlled Release*, 2008, **131**, 167–172.
- 103 J. T. Gonçalves, S. T. Schafer and F. H. Gage, *Cell*, 2016, **167**, 897–914.
- 104 M. Faiz, N. Sachewsky, S. Gascon, K. W. Bang, C. M. Morshead and A. Nagy, *Cell Stem Cell*, 2015, **17**, 624–634.
- 105 I. Kazanis, N. Gorenkova, J.-W. Zhao, R. J. M. Franklin, M. Modo and C. French-Constant, *Exp. Neurol.*, 2013, **248**, 387–397.



- 106 T. Zhao, T. Zhu, L. Xie, Y. Li, R. Xie, F. Xu, H. Tang and J. Zhu, *Transl. Stroke Res.*, 2022, **13**, 665–675.
- 107 B. Furie and B. C. Furie, *N. Engl. J. Med.*, 2008, **359**, 938–949.
- 108 G. K. Hansson, *N. Engl. J. Med.*, 2005, **352**, 1685–1695.
- 109 J. Loscalzo, *Pathophysiol. Haemostasis Thromb.*, 2002, **32**, 359–360.
- 110 J. H. Park, D. Dehaini, J. Zhou, M. Holay, R. H. Fang and L. Zhang, *Nanoscale Horiz.*, 2020, **5**, 25–42.
- 111 L. J. Rich and M. Seshadri, *Radiology*, 2015, **275**, 110–118.
- 112 K. Jansen, G. van Soest and A. F. van der Steen, *Ultrasound Med. Biol.*, 2014, **40**, 1037–1048.
- 113 B. L. Chung, M. J. Toth, N. Kamaly, Y. J. Sei, J. Becraft, W. J. Mulder, Z. A. Fayad, O. C. Farokhzad, Y. Kim and R. Langer, *Nano Today*, 2015, **10**, 759–776.
- 114 A. Hannah, G. Luke, K. Wilson, K. Homan and S. Emelianov, *ACS Nano*, 2014, **8**, 250–259.
- 115 N. J. Abbott, L. Ronnback and E. Hansson, *Nat. Rev. Neurosci.*, 2006, **7**, 41–53.
- 116 W. M. Pardridge, *Mol. Interventions*, 2003, **3**, 90–105, 190–151.
- 117 S. Ohtsuki and T. Terasaki, *Pharm. Res.*, 2007, **24**, 1745–1758.
- 118 R. Jin, G. Yang and G. Li, *Neurobiol. Dis.*, 2010, **38**, 376–385.
- 119 P. M. George and G. K. Steinberg, *Neuron*, 2015, **87**, 297–309.
- 120 X. Dong, *Theranostics*, 2018, **8**, 1481–1493.
- 121 M. F. Bennewitz and W. M. Saltzman, *Neurotherapeutics*, 2009, **6**, 323–336.
- 122 D. S. Jones and D. Q. M. Craig, *J. Pharm. Pharmacol.*, 2004, **56**, 1–2.
- 123 A. Mistry, S. Stolnik and L. Illum, *Int. J. Pharm.*, 2009, **379**, 146–157.
- 124 B. V. Zlokovic, *Neuron*, 2008, **57**, 178–201.
- 125 O. Kis, K. Robillard, G. N. Chan and R. Bendayan, *Trends Pharmacol. Sci.*, 2010, **31**, 22–35.
- 126 M. Simionescu, A. Gafencu and F. Antohe, *Microsc. Res. Tech.*, 2002, **57**, 269–288.
- 127 L. Crawford, J. Rosch and D. Putnam, *J. Controlled Release*, 2016, **240**, 251–266.
- 128 R. S. Pandya, L. Mao, H. Zhou, S. Zhou, J. Zeng, A. J. Popp and X. Wang, *Cent. Nerv. Syst. Agents Med. Chem.*, 2011, **11**, 81–97.
- 129 I. Brasnjevic, H. W. Steinbusch, C. Schmitz and P. Martinez-Martinez, *Prog. Neurobiol.*, 2009, **87**, 212–251.
- 130 I. L. Colao, R. Corteling, D. Bracewell and I. Wall, *Trends Mol. Med.*, 2018, **24**, 242–256.

